

Personalized Mood Prediction from Patterns of Behavior Collected with Smartphones

Brunilda Balliu*¹, Chris Douglas², Liat Shenhav³, Yue Wu³, Darsol Seok⁹, Doxa Chatzopoulou⁹, Bill Kaiser⁸, Victor Chen⁸, Jennifer Kim⁹, Sandeep Deverasetty⁹, Inna Arnaudova⁹, Robert Gibbons¹⁰, Eliza Congdon², Michelle G. Craske^{2,5}, Nelson Freimer^{2,6}, Eran Halperin^{3,7}, Sriram Sankararaman^{1,3,6}, Jonathan Flint^{2,6*}

Departments of ¹Computational Medicine, ²Psychiatry and Biobehavioral Science, ³Computer Science, ⁵Psychology, ⁶Human Genetics, ⁷Anesthesiology, ⁸Electrical Engineering and ⁹Semel Institute for Neuroscience and Human Behavior, University of California Los Angeles, Los Angeles, USA, ¹⁰Departments of Medicine, Public Health Sciences and Comparative Human Development, University of Chicago, USA

* Corresponding authors (emails: bballiu@ucla.edu and JFlint@mednet.ucla.edu)

Abstract

Over the last ten years, there has been considerable progress in using digital behavioral phenotypes, captured passively and continuously from smartphones and wearable devices, to infer mood and diagnose major depressive disorder. However, most digital phenotype studies suffer from poor replicability, often fail to detect clinically relevant events, and use measures of depression that are not validated or suitable for collecting large and longitudinal data. Here, we report high-quality longitudinal validated assessments of mood from computerized adaptive testing paired with continuous digital assessments of behavior from smartphone sensors for up to 40 weeks on 183 individuals experiencing mild to severe symptoms of depression. We apply a novel combination of cubic spline interpolation and idiographic models to generate individualized predictions of future mood from the digital behavioral phenotypes, achieving high prediction accuracy of depression severity up to three weeks in advance ($R^2 \geq 80\%$). We show that the passive behavioral phenotypes enhance prediction of future mood over and above a baseline model which predicts future mood based on past depression severity alone for 52% of individuals in our cohort. In conclusion, our study verified the feasibility of obtaining high-quality longitudinal assessments of mood from a clinical population and predicting symptom severity weeks in advance using passively collected digital behavioral data. Our results indicate the possibility of expanding the repertoire of patient-specific behavioral measures to enable future psychiatric research.

Introduction

Major depressive disorder (MDD) affects almost one in five people¹ and is now the world's leading cause of disability². However, it is often undiagnosed: only about half of those with MDD are identified and offered treatment^{3,4}. In addition, for many people, MDD is a chronic condition characterized by periods of relapse and recovery that requires ongoing monitoring of symptoms. MDD diagnosis and symptom

monitoring is typically dependent on clinical interview, a method that rarely exceeds an inter-rater reliability of 0.7⁵; in one large field study reliability was estimated to be as low as 0.25⁶. Furthermore, sufferers are unlikely to volunteer that they are depressed because of the reduced social contact associated with low mood and because of the stigma attached to admitting to being depressed. Developing new ways to quickly and accurately diagnose MDD or monitor depressive symptoms in real time, without personal interviews, and hence provide therapy, would substantially alleviate the burden of this common and debilitating condition.

The advent of electronic methods of collecting information, e.g., smartphone sensors or wearable devices, means that behavioral measures can now be obtained in real time as individuals go about their daily lives. Over the last ten years there has been considerable progress in using these digital behavioral phenotypes to infer mood and depression⁷⁻²². Yet, most digital mental health studies suffer from one or more of the following limitations²³⁻²⁵. First, many studies use less than a hundred¹⁰ and some even a handful of participants^{12,26,27}. Studies with small samples have poor replicability¹⁸. We found only two studies with sample sizes in the hundreds^{20,28}. Second, most studies do not have access to sufficient longitudinal data to detect changes within an individual^{10,11,26,29}, even though such changes are highly informative for clinical care. The few studies with longitudinal assessments use ecological momentary assessments^{20,26,27} to measure state mood, rather than a psychometrically validated symptom scale for depression. Furthermore, they examine associations between behavior and mood at a population level²⁰. This nomothetic approach is limited by the fact that both mood and its relationship to behavior can vary substantially between individuals. Last, many of the existing studies focus on healthy subjects, thus prohibiting evaluation of how well digital phenotypes perform in predicting depression³⁰.

Here, we overcome these limitations by using a validated measure of depression from computerized adaptive testing³¹ to obtain high-quality longitudinal measures of mood and smartphone

sensing³² to passively and continuously collect behavioral phenotypes for up to 40 weeks on 183 individuals experiencing mild to severe symptoms of depression (3,005 days with mood assessment and 29,254 days with behavioral assessment). In addition, we use an idiographic (or, personalized) modelling approach to predict future mood weeks in advance and provide individual-specific predictors of depression trajectories. As a benchmark for the performance of our approach, we compare the predictive performance with that of a baseline model, which predicts based on past depression severity alone, a conventional nomothetic approach, which uses a population-based prediction model, and a modification of the nomothetic approach which accounts for the individual specificity of mood. Ultimately, we expect that this approach can provide patient-specific predictors of depressive symptom severity that can be used to guide personalized intervention, as well as enable future psychiatric research, e.g., genome and phenome-wide association studies.

Results

Study participants and treatment protocol

Participants (N = 437; 76.5% female, 26.5% white) are University of California Los Angeles (UCLA) students experiencing mild to severe symptoms of depression or anxiety enrolled as part of the Screening and Treatment for Anxiety and Depression^{33–35} (STAND) study (Sup Figure 1). Participants are initially assessed using the Computerized Adaptive Testing Depression Inventory³¹ (CAT-DI), an online adaptive tool that offers validated assessments of depression severity (measured on a 0-100 scale). After the initial assessment, participants are routed to appropriate treatment resources depending on depression severity: those with mild ($35 \leq \text{CAT-DI} < 65$) to moderate ($65 \leq \text{CAT-DI} < 75$) depression at baseline received online support with or without peer coaching³⁶ while those with severe depression ($\text{CAT-DI} \geq 75$) received in-person care from a clinician (Online Methods).

STAND enrolled participants in two waves, each with different inclusion criteria and CAT-DI assessment and treatment protocol (Sup Figure 2A). Wave 1 was limited to individuals with mild to moderate symptoms at baseline (N=182) and treatment lasted for up to 20 weeks. Wave 2 included individuals with mild to moderate (N=142) and severe (N=124) symptoms and treatment lasted for up to 40 weeks. Eleven individuals participated in both waves. Depression symptom severity was assessed up to every other week for the participants that received online support (both waves), i.e., those with mild to moderate symptoms, and every week for the participants that received in-person clinical care, i.e., those with severe symptoms.

Adherence to CAT-DI assessment protocol

In total, participants provided a total of 4,507 CAT-DI assessments (out of 11,218 expected by the study protocols). Participant adherence to CAT-DI assessments varied across the treatment groups (Likelihood ratio test [LRT] P-value $< 2.2 \times 10^{-16}$), enrollment waves (LRT P-value = 2.86×10^{-6}), and during the follow-up period (LRT P-value = 1.29×10^{-6}). Specifically, participants that received clinical care were more adherent than those which only received online support (Sup Figure 2A). Attrition for participants which received clinical care was linear over the follow-up period, with 1.7% of participants dropping out CAT-DI assessments within two weeks into the study. Attrition for participants that received online support was large two weeks into the study (33.5% of Wave 1 and 37.3% of Wave 2 participants) and linear for the remaining of the study.

For building personalized mood prediction models, we focus on 183 individuals (49 from Wave 1 and 134 from Wave 2) who had at least five mental health assessments during the study (Online Methods). For these individuals we obtained a total of 3,005 CAT-DI assessments with a median of 13 assessments, 171 follow-up days, and 10 days between assessments per individual (Figure 1A-C).

Computerized adaptive testing captures treatment-related changes in depression severity

We assessed what contributes to variation in the CAT-DI severity scores (Figure 1E). Subjects are assigned to different treatments (online with or without coaching and clinical care) depending on their CAT-DI severity scores, so not surprisingly we see a significant source of variation attributable to the treatment group (6.43% of variance explained, 95% CI: 5.20 - 9.40%, Online Methods). Once assigned to a treatment group, we expect to see changes over time as treatment is delivered. This is reflected in a significant source of variation attributable to the number of weeks spent in the study (10.87% of variance explained, 95% CI: 9.39 - 12.79%) and the improved scores for individuals with severe symptoms at baseline as they spend more time in the study (Sup Figure 3). We found no statistically significant effect of the COVID pandemic, sex, and other study parameters. The largest source of variation in depression severity scores is attributable to between-individual differences (42.26% of variance explained, 95% CI: 38.47 - 42.55%), suggesting that accurate prediction of CAT-DI severity requires learning models tailored to each individual.

Digital behavioral phenotypes capture changes in behavior

We set out to examine how digital behavioral phenotypes change over time for each person and with CAT-DI severity scores. For example, we want to know how hours of sleep on a specific day for a specific individual differs from the average hours of sleep in the previous week, or month. To answer these questions, we extracted digital behavioral phenotypes (referred to hereinafter as features) captured from participants' smartphone sensors and investigated which features predicted the CAT-DI scores. STAND participants had the AWARE framework³² installed on their smartphones, which queried phone sensors to obtain information about a participant's location, screen on/off behavior, and number of incoming and outgoing text messages and phone calls. We processed these measurements (Online methods) to obtain

daily aggregate measures of activity (23 features), social interaction (18 features), sleep quality (13 features), and device usage (two features). In addition, we processed these features to capture relative changes in each measure for each individual, e.g., changes in average amount of sleep in the last week compared to what is typical over the last month. In total, we obtained 1,325 features (Online methods). Missing daily feature values (Sup Figure 4) were imputed (Online Methods), resulting in 29,254 days of logging events across all individuals.

Several of these features map onto the DSM-5 MDD criteria of anhedonia, sleep disturbance, and loss of energy (Supplemental Methods; Sup Figure 5). We found that these features in some cases do indeed correlate with changes in depression: Figure 2 illustrates an individual with severe depressive symptoms for whom we can identify a window of disrupted sleep that co-occurred with a clinically significant increase in symptom severity (from mild to severe CAT-DI scores). Subsequently, a return to baseline patterns of sleep coincided with symptom reduction. Quantifying this relationship poses a number of issues, which we turn to next.

Predicting CAT-DI scores from digital phenotypes

To predict future depression severity scores using digital behavioral phenotypes, we considered three analytical approaches. First, we applied an idiographic approach, whereby we build a separate prediction model for each of the participants. Specifically, for each individual, we train an elastic net linear regression model using the first 70% of their depression scores and predict the remaining 30% of scores. Second, we applied a nomothetic approach that used data from all participants to build a single model for depression severity prediction using the same analytical steps: we train an elastic net regression model using the first 70% of depression scores of each individual and predict the remaining 30% of scores

(Online Methods). The result of this nomothetic approach was a single elastic net regression model that makes predictions in all participants.

The main difference between the nomothetic and idiographic approach is that the nomothetic model assumes that each feature has the same relationship with the CAT-DI scores across individuals, for example, that a phone interaction is always associated with an increase in depression score. However, it is possible, and we see this in our data, that an increase in phone interaction can be associated with an increase in symptom severity for one person, but a decrease in another (Sup Figure 6). The idiographic model allows for this possibility by using a different slope for each feature and individual. In addition, we know that large differences exist in average depression scores between individuals (Figure 1E). To understand the impact of accounting for these differences in a nomothetic approach, we also applied a third approach (referred to as nomothetic*) which includes individual indicator variables in the elastic net regression model in order to allow for potentially different intercepts for each individual.

To assess whether digital behavioral phenotypes predict mood, we have to deal with the problem that digital phenotypes are acquired daily, while CAT-DI are usually administered every week (and often much less frequently, on average every 10 days). We assume that the CAT-DI indexes a continuously variable trait, but what can we use as the target for our digital predictions when we have such sparsely distributed measures? We can treat this as a problem of imputation, in which case the difficulty reduces to knowing the likely distribution of missing values. However, we also assume that both CAT-DI and digital features only imperfectly reflect a fluctuating latent trait of depression. Thus, our imputation is used not only to fill in missing data points but also to be a closer reflection of the underlying trait that we are trying to predict, namely, depressive severity.

We interpolate the unmeasured estimates of depression by modeling the latent trait as a cubic spline with different degrees of freedom (Figure 3A). For many individuals, CAT-DI values fluctuate

considerably during the study, while for others less so. To accommodate this variation, we alter the degrees of freedom of the cubic spline: the more degrees of freedom, the greater the allowed variation. For each individual, we used cubic splines with four degrees of freedom, denoted by CS(4df), degrees of freedom corresponding to the number of observed CAT-DI categories in the training set, denoted by CS(2-4df), and degrees of freedom identified by leave-one-out cross-validation in the training set, denoted by CS(cv). For comparison purposes, we also used a last-observation-carried-forward (LOCF) approach, a naive interpolation method which does not apply any smoothness to the observed trait. Because spline interpolation will cause data leakage across the training-testing split and upwardly bias prediction accuracy, we train our prediction models using cubic spline interpolation on only the training data (first 70% of time series of each individual) and assess prediction accuracy performance in the testing set (last 30%) using the time series generated by applying cubic splines to the entire time series (Figure 3B).

We evaluated the prediction performance of each model and for each latent trait across and within participants. We refer to the former as group level prediction and the later as individual level prediction. Looking at group level prediction performance, compared to within each participant separately, allows us to compute prediction accuracy metrics, e.g., R^2 , and test for their statistical significance across all predicted observations. In addition, it allows us to study prediction accuracy as a function of how many days ahead we are predicting.

We first evaluated group level prediction accuracy. Figure 4A and Sup Figure 7 show group level prediction performance for each latent trait using the nomothetic, nomothetic*, and idiographic models. We observed that across all latent traits the nomothetic model shows very poor prediction accuracy ($R^2 < 5\%$ for all latent traits), compared to the nomothetic* ($R^2 = 41-59\%$) or idiographic ($R^2 = 41-67\%$) models. This is in line with the large proportion of depression scores variance explained by between-individual differences (Figure 1E) which get best captured by the nomothetic* and idiographic models. We also

compared the prediction performance for each of the different latent traits. We achieve a higher prediction accuracy for the cubic spline latent traits compared to the LOCF latent trait. For example, for the idiographic models, we obtained an $R^2 = 67.95\%$ for CS(2-4df) versus 41.34% for LOCF, implying that weekly patterns of depression severity, which are more likely to be captured by the LOCF latent trait, are harder to predict than depression severity patterns over a couple of weeks or months, which are more likely to be captured by the cubic spline latent traits with smallest degrees of freedom.

To understand the effect of time on prediction accuracy, we assessed prediction performance as a function of the number of days ahead we are predicting from the last observation in the training set (Figure 4B). The idiographic models achieved high prediction accuracy for depression scores up to three weeks from the last observation in the training set, e.g., $R^2 = 91.0\%$ and 79.7% for the CS(2-4df) latent trait to predict observations one week and three weeks ahead, respectively. Prediction accuracy falls below 80% after four weeks.

We next evaluated individual level prediction accuracy. For this analysis, in order to be able to assess the statistical significance of our prediction accuracy within each individual, we only keep individuals with at least five mental health assessments in the test set ($N=139$). In accordance with the group level prediction performance, the idiographic model outperformed the other models at the individual level. Using an idiographic modelling approach, we significantly predicted the future mood for 65.5% of individuals (91 out of 139 with $R > 0$ and $FDR \leq 5\%$ across individuals) for at least one of the latent traits (Figure 5A and Sup Figure 9), compared to 46.0% and 46.8% of individuals for the nomothetic and nomothetic* model, respectively. The median R^2 value across significantly predicted individuals for the idiographic models was 57.5% (Figure 5B and Sup Figure 10), compared to 31.7% and 35.9% for the nomothetic and nomothetic* model, respectively. In addition, for thirty-eight of these individuals, the idiographic model had prediction accuracy greater than 70%, demonstrating high

predictive power in inferring mood from digital behavioral phenotypes for these individuals, compared to 13 and 9 for the nomothetic and nomothetic* model, respectively (Figure 5B and Sup Figure 10).

To identify the features that most robustly predict depression in each person we extracted top-feature predictors for each individual's best-fit idiographic model. We limit this analysis to the 91 individuals which showed significant prediction accuracy for at least one of the latent traits. Although no feature uniformly stood out, the variation within the last 30 days in the proportion of unique contacts for outgoing texts and messages (a proxy for social interaction), the time of first interaction with phone in the morning (a proxy for wake up time and sleep quality), and the proportion of time spent at home during the day (a proxy for activity level) were among the top predictors of future mood (Figure 6). The heatmap display of predictor importance highlights the heterogeneity of passive features for predicting the future across individuals. For example, poor mental health, as indicated by high CAT-DI depression severity scores, was associated with decreased variation in the hours the phone was off between midnight and 8 a.m. (a proxy for hours of sleep and sleep quality) in the past 30 days for one individual while for another individual it was associated with increased variation.

Evaluation of feature contribution to prediction performance

So far, our models are all of the form $\text{mood} \sim \alpha + \beta * \text{phone features}$. This model implies that if the phone feature has no predictive accuracy, we may still be able to predict something about the future mood of an individual in the test set by using that individual's stable (i.e., mean) mood in the training set, reflected by the value of 'alpha', the intercept. We assessed to what extent adding the phone features improves the prediction of the idiographic models above that achieved by a baseline model that includes just the intercept (i.e., $\text{mood} \sim \alpha$). In order to do that, we first identified the best fitting latent trait for each individual according to the idiographic model with features and compare that model to the

equivalent baseline idiographic model without features in terms of prediction mean absolute error (MAE). Within each individual, the baseline idiographic model always predicts the same value, i.e., alpha, so we cannot compute R^2 metrics for the baseline model. As above, we limit this analysis to the individuals with at least five mental health assessments in the test set (N=139).

The feature-based model performed significantly better than the baseline model (Figure 7A, one sided Wilcoxon signed-rank test, p-value = 3.33×10^{-2}) with a median decrease in MAE of 4.43% across all 139 individuals. The feature-based model reduced the MAE compared to a baseline model for 52% of individuals (70 out of 139) with 48 individuals having a decrease in the MAE of at least 20%. Figure 7B illustrates the prediction performance for one such individual in our study. These results suggest that the passive phone features enhance prediction, over and above past CAT-DI, for a subset of individuals.

Factors associated with prediction performance

Using digital behavioral features to predict future mood was useful for about half of our cohort and the contribution of the features to the prediction performance varies across these individuals. What might contribute to this variation? Identifying the factors involved might allow us to develop additional models with higher prediction accuracy. To identify factors that are associated with prediction performance, we computed the correlation between accuracy metrics (prediction R^2 and MAE of feature-based model and difference in MAE between feature-based and baseline models) with different study parameters e.g., treatment group, sex, etc. (Figure 8). Larger differences in median depression scores between the training and test set for each individual were correlated with poorer prediction performance, as measured by MAE (Spearman's $\rho=0.65$, p-value = 3.46×10^{-11}). This suggests that, for many of the individuals in the study, the training depression scores are not as representative of the test depression scores, e.g., if individuals have high CAT-DI in the training but low CAT-DI in the test. Indeed, this is the case for most individuals

in our cohort who are in treatment that improves their symptoms during the course of the study (Sup Figure 3). The size of the training and test set as well as demographic variables were not strongly correlated to prediction performance. While we had poorer prediction performance for individuals whose mood changes between the training and test set, these are also the individuals for which using a feature-based model improves prediction accuracy compared to a baseline model that predicts based on past depression severity alone. Larger differences in median depression scores between the training and test set for each individual were correlated with better prediction performance of a feature-based model, compared to a baseline model (Spearman's $\rho=0.54$, $p\text{-value} = 1.53 \times 10^{-7}$).

Discussion

In this paper, we showed the feasibility of longitudinally measuring depressive symptoms over 183 individuals for up to 10 months using computerized adaptive testing and passively and continuously measuring behavioral data captured from the sensors built into smartphones. Using a novel combination of cubic spline interpolation and idiographic prediction models, we were able to impute and predict a latent depression trait on a hold-out set of each individual several weeks in advance.

Our ability to longitudinally assess depressive symptoms and behavior within many individuals and over a long period of time enabled us to assess how far out we can predict depressive symptoms, how variable prediction accuracy can be across different individuals, and what factors contribute to this variability. In addition, it enabled us to assess the contribution of behavioral features to prediction accuracy above and beyond that of prior symptom severity alone. We observed that prediction accuracy dropped below 70% after three weeks. In addition, prediction accuracy varied considerably across individuals as did the contribution of the features to this accuracy. Individuals with large changes in symptom severity during the course of the study (such as those in clinical care) were harder to predict but benefited the most from using behavioral features. We expect that pairing digital phenotypes from

smartphones with behavioral phenotypes from wearable devices, which are worn continuously and might measure behavior with less error, as well as addition of phenotypes, like those from electronic health records, could help address some of these challenges.

Our results are consistent with other studies that predict daily mood as measured by ecological momentary assessments or a short screener (i.e., PHQ2²⁴) and confirm the superior prediction performance of idiographic models over nomothetic ones. Our study goes further, by exploring if the superior prediction accuracy of idiographic models is a result of better modeling the relationship between features and mood or simply of better modeling the baseline mood of each individual. We show that a large part of the increase in prediction performance of idiographic models is due to the latter, as indicated by the increase in prediction performance between the nomothetic and modified nomothetic models.

High-burden studies over long time periods may result in drop-out, particularly for depressed individuals³⁷. In our case, we observed that attrition for CAT-DI assessment was linear over the follow-up period, except for the first two weeks during which a large proportion of individuals which received online support dropped out (typical of online mental health studies³⁸). In addition, participants which received clinical care were more adherent than those which received online support, despite endorsing more severe depressive symptoms. These participants had regular in-person treatment sessions during which they were instructed to complete any missing assessments emphasizing the importance of using reminders or incentives for online mental health studies.

There are several limitations in the current study. First, the idiographic models that we use here might not thus maximize statistical power. In addition, they assume a linear relationship between behavioral features and depression severity and will fit poorly if this assumption is violated. One potential alternative is to employ mixed models that jointly model data from all individuals using individual-specific slopes and low degree polynomials. However, due to the high dimensionality of our data such

models are hard to implement. Second, the adaptive nature of CAT-DI, which might assess different symptoms for different individuals, frustrates joint analyses. Finally, the age and gender distribution in our participants may limit the generalizability of our findings to the wider population.

In conclusion, our study verified the feasibility of using passively collected digital behavioral phenotypes from smartphones to predict depressive symptoms weeks in advance. Its key novelty lies in the use of computerized adaptive testing, which enabled us to obtain high-quality longitudinal assessments of mood on 183 individuals over many months, and in the use of personalized prediction models, which offer a much higher predictive power compared to nomothetic models. Ultimately, we expect that the method will lead to a screening and detection system that will alert clinicians in real-time to initiate or adapt treatment as required. Moreover, as passive phenotyping becomes more scalable for hundreds of thousands of individuals, we expected that this method will enable large genome and phenome-wide association studies for psychiatric genetic research.

Materials and methods

Study participants and protocol

Participants are University of California Los Angeles (UCLA) students experiencing mild to severe symptoms of depression or anxiety enrolled as part of the STAND program developed under the UCLA Depression Grand Challenge³⁵ treatment arm. All participants provided written informed consent for the study protocol approved by the UCLA institutional review board (IRB #16-001395 for those receiving online support and #17-001365 for those receiving clinical support). All groups are offered behavioral health tracking through the AWARE³² framework and had to install the app in order to participate in the study. STAND enrolled participants in two waves. The first wave enrolled participants from April 2017 to June 2018. The second wave of enrollment began at the start of the academic year in 2018 and continued

for three years, during which time, from March 2020, a Safer-At-Home order was imposed in Los Angeles to control the spread of COVID-19.

Depression symptom severity was assessed using the Computerized Adaptive Testing Depression Inventory³¹ (CAT-DI), a validated online mental health tracker. Computerized adaptive testing is a technology for interactive administration of tests that tailors the test to the patient³⁹. Tests are 'adaptive' in the sense that the testing is driven by an algorithm that selects questions in real-time and in response to the ongoing responses of the patient. CAT-DI uses item response theory to select a small number of questions from a large bank, thus providing a powerful and efficient way to detect psychiatric illness without suffering response fatigue.

Depression symptom severity was assessed up to every other week for the participants that received online support (both waves), i.e., those with mild to moderate symptoms, and every week for the participants that received in-person clinical care, i.e., those with severe symptoms (Sup Figure 2A). Participants that received in-person care had also four in-person assessment events, at weeks 8, 16, 28, and 40, prior to the COVID-19 pandemic. Thus, Wave 1 participants can have a maximum of 13 CAT-DI assessments while Wave 2 participants can have a maximum of 21 (online support) or 44 assessments, depending on severity and excluding initial assessments prior to treatment assignment.

CAT-DI was assessed at least one time for 437 individuals that installed the AWARE app. Here, we limit our prediction analyses to individuals that have at least five CAT-DI assessments (N=238; since we need at least four points to interpolate CAT-DI in the training set), have at least 60 days of sensor data in the same period for which CAT-DI data is also available (N=189), and show variation in their CAT-DI scores in the training set (N=183), which is necessary in order to build prediction models.

Overview of the treatment protocol

STAND use computerized adaptive testing to initially assess depressive mood severity at entry, from which students are routed to appropriate treatment resources. Individuals who are not currently experiencing symptoms of depression or anxiety are offered the opportunity to participate in the study with an active treatment component by contributing CAT-DI assessment. These individuals are excluded from our analyses as they do not show any variation in CAT-DI. Individuals who are mildly depressed or anxious or at risk for depression or anxiety are provided internet-based cognitive behavior therapy, which includes adjunctive support provided by trained peers or clinical psychology graduate students via video chat or in person. Individuals who are severely depressed, suicidal, or bipolar/manic and who need more intensive treatment, are offered an evaluation within the STAND clinic, including individualized treatment by a team of psychiatrists and psychologists.

Feature extraction from smartphone sensors

We describe feature extraction in detail in the supplement. Broadly, we extracted 23 features related to mobility, e.g., location entropy, 13 related to sleep and circadian rhythm, e.g., hours of uninterrupted sleep, 18 related to social interaction, e.g., duration of outgoing calls, and two related to mobile device usage, e.g., number of interactions with phone per day. Each of these features was calculated on a daily basis. Furthermore, each of these features was computed over three daily non-overlapping time windows of equal duration (night 00:00-08:00, day 08:00-16:00, evening 16:00-00:00), under the hypothesis that participant behavior may be more or less variable based on external constraints such as a regular class schedule during daytime hours.

In addition, considering a participant's current mental state may be influenced by patterns of behavior from days prior, sliding window averages of each of the daily features were

calculated over multiple sliding windows ranging from three days to one month prior to the current day, i.e., windows of length three, seven, 14, and 30 days. The variance of each feature was also calculated over these same windows, to estimate whether behavior had been stable or variable during that time, e.g., were there large fluctuations in sleep time over the past week?

Finally, under the hypothesis that recent *changes* in behavior may be more indicative of changes in mental state than absolute measures, a final set of transformations were applied to each feature. These transformations compared the sliding window means of two different durations against each other, to estimate the change in behavior during one window over that of a longer duration window (the longer window serving as a local baseline for the participant). This allowed estimates from the raw features of whether, e.g., the participant had slept less last night than typical over the past week or slept less on average in the last week than typical over the last month. All of these transformations were applied to the base features extracted from sensor data and included as separate features fed into subsequent regression approaches.

In total, 1,325 raw and transformed features were extracted and included in the final analysis.

Imputation of smartphone-based features

To address the missing features problem (Sup Figure 4), we considered two different imputation methods: matrix completion via iterative soft-thresholder SVD as implemented in the R package `softImpute`⁴⁰ and cubic spline interpolation with degrees of freedom equal to the number of days an individual participated in the study (to achieve the least amount of smoothing). Both approaches were applied separately to each individual. The former was applied across all features while the latter was applied separately to each feature. In the main text, we discuss results based on features imputed using

cubic interpolation, which achieved the best prediction accuracy. We show results based on matrix completion interpolation in Sup Figure 8. When fitting prediction models without imputation of missing feature data, we remove days with more than 90% of features missing (within each individual for individual-level models and across individuals for the population-level model) and features that are missing for more than 90% of the days for which the individual(s) participated in the study. Before prediction, we normalize all features to have zero mean and unit standard deviation.

Variance partition of CAT-DI metrics

We calculate the proportion of CAT-DI severity variance explained by different study parameters using a linear mixed model as implemented in the R package `variancePartition`⁴¹ with the subject id, study id, season, sex, and year modeled as random variables while the day of the study, the age of the subject, and a binary variable indicating the dates before or after the safer at home order was issued in California modeled as fixed, i.e.,

$$y = \sum_j X_j \beta_j + \sum_k Z_k a_k + \epsilon$$

where y is the vector of the CAT-DI values across all subjects and time points, X_j is the matrix of j^{th} fixed effect with coefficients β_j , Z_k is the matrix corresponding to the k^{th} random effect with coefficients a_k drawn from a normal distribution with variance $\sigma_{a_k}^2$. The noise term, ϵ , is drawn from a normal distribution with variance σ_ϵ^2 . All parameters are estimated with maximum likelihood⁴². Variance terms for the fixed effects are computed using the post hoc calculation $\hat{\sigma}_{\beta_j}^2 = \text{var}(X_j \beta_j)$. The total variance is $\hat{\sigma}_{Total}^2 = \hat{\sigma}_{\beta_j}^2 + \hat{\sigma}_{a_k}^2 + \hat{\sigma}_\epsilon^2$ so that the fraction of variance explained by the j^{th} fixed effect is $\hat{\sigma}_{\beta_j}^2 / \hat{\sigma}_{Total}^2$, by the k^{th} random effect is $\hat{\sigma}_{a_k}^2 / \hat{\sigma}_{Total}^2$, and the residual variance is $\hat{\sigma}_\epsilon^2 / \hat{\sigma}_{Total}^2$. Confidence intervals for

variance explained were calculated using parametric bootstrap sampling as implemented in the R package `variancePartition`⁴¹.

Imputation and of CAT-DI severity scores

To get daily-level data, we interpolate the CAT-DI severity scores for each individual across the whole time series (ground truth) or only the time series corresponding to the training set (70% of the time series) by moving the last CAT-DI score forward, denoted by LOCF, or by smoothing the CAT-DI scores using cubic splines with different degrees of freedom (Figure 3A). Cubic smoothing spline fitting was done using the `smooth.spline` function from the `stats` package in R. We consider cubic splines with four degrees of freedom (denoted by CS(4df) and corresponding to the number of possible CAT-DI severity categories, i.e. normal, mild, moderate, and severe), cubic splines with degrees of freedom equal to the number of observed CAT-DI categories for each individual in the training set (ranging from two to four and denoted by CS(2-4df)), and degrees of freedom identified by ordinary leave-one-out cross-validation in the training set (denoted by CS(cv)).

Nomothetic and idiographic prediction of mood

We split the data for each individual into a training (70% of trajectory) and a test set (remaining 30% of trajectory). To predict the future mood of each individual in the test set from smartphone-based features in the test set, we train an elastic net linear regression model⁴³ in the train set. We set α , i.e., the mixing parameter between ridge regression and lasso, to 0.5 and use 10-fold cross-validation to find the value for parameter λ , i.e., the shrinkage parameter. For the idiographic models, we train separate elastic net models for each individual while for the nomothetic and modified nomothetic models we train one model across all individuals. To account for individual differences in the average CAT-DI severity scores

in the training set, the modified nomothetic model fits individual-specific intercepts by including individual indicator variables in the regression model. This is similar in nature to a random intercept mixed model where each individual has their own intercept. Note that the test data are the same for all of these models, i.e., the remaining 30% of each individual's trajectories. Predictions outside the CAT-DI severity range, i.e., [0,100], are set to NA and not considered for model evaluation. We compute prediction accuracy metrics by computing the Pearson's product-moment correlation coefficient (R) between observed and predicted depression scores in the test set across and within individuals as well as the squared Pearson coefficient (R^2). To assess the significance of the prediction accuracy we use a one-sided paired test for Pearson's product-moment correlation coefficient, as implemented in the *cor.test* function of the stats⁴⁴ R package, and a likelihood ratio test for the significance of R^2 . We use the Benjamini-Hochberg procedure⁴⁵ to control the false discovery rate across individuals at 5%.

Acknowledgments

The authors gratefully acknowledge all study participants. S.S was funded in part by NIH grant R35GM125055 and NSF grants III-1705121 and CAREER-1943497. DS was supported by NSF-NRT #1829071.

Author Contributions

BB and JF conceived of the project. D.C., V.C., and J.K. participated in the subject recruitment and data collection. BB lead the data analysis with contributions from CD, LS, AW, and DS. BB and JF wrote the first draft of the manuscript with contribution from CD and SS. All authors contributed to subsequent edits of the manuscript and approved the final manuscript.

Competing Interests

The authors declare no competing interests.

Data and Code Availability

The datasets generated and analyzed during the current study are available from the corresponding author on reasonable request. The code that supports the findings of this study is available online at https://github.com/BrunildaBalliu/stand_mood_prediction.

References

1. Hasin, D. S. *et al.* Epidemiology of Adult DSM-5 Major Depressive Disorder and Its Specifiers in the United States. *JAMA Psychiatry* **75**, 336–346 (2018).
2. World Health Organization. Depression and Other Common Mental Disorders: Global Health Estimates. Preprint at (2017).
3. Goldberg, D. Epidemiology of mental disorders in primary care settings. *Epidemiol Rev* **17**, 182–190 (1995).
4. Wells, K. B. *et al.* Detection of depressive disorder for patients receiving prepaid or fee-for-service care. Results from the Medical Outcomes Study. *JAMA* **262**, 3298–3302 (1989).
5. Spitzer, R. L., Forman, J. B. & Nee, J. DSM-III field trials: I. Initial interrater diagnostic reliability. *Am J Psychiatry* **136**, 815–817 (1979).
6. Regier, D. A. *et al.* DSM-5 field trials in the United States and Canada, Part II: test-retest reliability of selected categorical diagnoses. *Am J Psychiatry* **170**, 59–70 (2013).
7. Madan, A., Cebrian, M., Lazer, D. & Pentland, A. Social sensing for epidemiological behavior change. *MIT web domain* (2010).
8. Ma, Y., Xu, B., Bai, Y., Sun, G. & Zhu, R. Daily Mood Assessment Based on Mobile Phone Sensing. in *2012 Ninth International Conference on Wearable and Implantable Body Sensor Networks* 142–147 (2012). doi:10.1109/BSN.2012.3.
9. Chen, Z. *et al.* Unobtrusive sleep monitoring using smartphones. in *2013 7th International Conference on Pervasive Computing Technologies for Healthcare and Workshops* 145–152 (2013).
10. Likamwa, R., Liu, Y., Lane, N. & Zhong, L. MoodScope: Building a Mood Sensor from Smartphone Usage Patterns. in (2013). doi:10.1145/2462456.2464449.

11. Frost, M., Doryab, A., Faurholt-Jepsen, M., Kessing, L. & Bardram, J. Supporting disease insight through data analysis: Refinements of the MONARCA self-assessment system. *UbiComp 2013 - Proceedings of the 2013 ACM International Joint Conference on Pervasive and Ubiquitous Computing* (2013) doi:10.1145/2493432.2493507.
12. Doryab, A., Min, J.-K., Wiese, J., Zimmerman, J. & Hong, J. I. Detection of Behavior Change in People with Depression. in (2019).
13. Lane, N. *et al.* BeWell: Sensing Sleep, Physical Activities and Social Interactions to Promote Wellbeing. *Mobile Networks and Applications* **19**, 345–359 (2014).
14. Wang, R. *et al.* StudentLife: Assessing mental health, academic performance and behavioral trends of college students using smartphones. in (2014).
doi:10.1145/2632048.2632054.
15. Saeb, S. *et al.* Mobile Phone Sensor Correlates of Depressive Symptom Severity in Daily-Life Behavior: An Exploratory Study. *J Med Internet Res* **17**, e175 (2015).
16. Canzian, L. & Musolesi, M. Trajectories of depression: unobtrusive monitoring of depressive states by means of smartphone mobility traces analysis. in 1293–1304 (2015).
doi:10.1145/2750858.2805845.
17. Saeb, S., Lattie, E. G., Schueller, S. M., Kording, K. P. & Mohr, D. C. The relationship between mobile phone location sensor data and depressive symptom severity. *PeerJ* **4**, e2537 (2016).
18. Asselbergs, J. *et al.* Mobile Phone-Based Unobtrusive Ecological Momentary Assessment of Day-to-Day Mood: An Explorative Study. *J Med Internet Res* **18**, e72 (2016).

19. DeMasi, O., Feygin, S., Dembo, A., Aguilera, A. & Recht, B. Well-Being Tracking via Smartphone-Measured Activity and Sleep: Cohort Study. *JMIR Mhealth Uhealth* **5**, e137 (2017).
20. Servia-Rodríguez, S. *et al.* Mobile Sensing at the Service of Mental Well-being: a Large-scale Longitudinal Study. in *Proceedings of the 26th International Conference on World Wide Web* 103–112 (International World Wide Web Conferences Steering Committee, 2017). doi:10.1145/3038912.3052618.
21. Sarda, A., Munuswamy, S., Sarda, S. & Subramanian, V. Using Passive Smartphone Sensing for Improved Risk Stratification of Patients With Depression and Diabetes: Cross-Sectional Observational Study. *JMIR Mhealth Uhealth* **7**, e11041 (2019).
22. Smuck, M., Odonkor, C. A., Wilt, J. K., Schmidt, N. & Swiernik, M. A. The emerging clinical role of wearables: factors for successful implementation in healthcare. *npj Digit. Med.* **4**, 1–8 (2021).
23. Aledavood, T. *et al.* Smartphone-Based Tracking of Sleep in Depression, Anxiety, and Psychotic Disorders. *Curr Psychiatry Rep* **21**, 49 (2019).
24. De Angel, V. *et al.* Digital health tools for the passive monitoring of depression: a systematic review of methods. *npj Digit. Med.* **5**, 1–14 (2022).
25. Zarate, D., Stavropoulos, V., Ball, M., de Sena Collier, G. & Jacobson, N. C. Exploring the digital footprint of depression: a PRISMA systematic literature review of the empirical evidence. *BMC Psychiatry* **22**, 421 (2022).
26. Shah, R. V. *et al.* Personalized machine learning of depressed mood using wearables. *Transl Psychiatry* **11**, 1–18 (2021).

27. Jacobson, N. C. & Bhattacharya, S. Digital biomarkers of anxiety disorder symptom changes: Personalized deep learning models using smartphone sensors accurately predict anxiety symptoms from ecological momentary assessments. *Behaviour Research and Therapy* **149**, 104013 (2022).
28. Pratap, A. *et al.* The accuracy of passive phone sensors in predicting daily mood. *Depression and Anxiety* **36**, 72–81 (2019).
29. Burns, R. A., Anstey, K. J. & Windsor, T. D. Subjective well-being mediates the effects of resilience and mastery on depression and anxiety in a large community sample of young and middle-aged adults. *Aust N Z J Psychiatry* **45**, 240–248 (2011).
30. Stachl, C. *et al.* Predicting personality from patterns of behavior collected with smartphones. *PNAS* **117**, 17680–17687 (2020).
31. Gibbons, R. D., Weiss, D. J., Frank, E. & Kupfer, D. Computerized Adaptive Diagnosis and Testing of Mental Health Disorders. *Annual Review of Clinical Psychology* **12**, 83–104 (2016).
32. Ferreira, D., Kostakos, V. & Dey, A. K. AWARE: Mobile Context Instrumentation Framework. *Frontiers in ICT* **2**, (2015).
33. UCLA Depression Grand Challenge | Screening and Treatment for Anxiety & Depression (STAND) Program. <https://www.stand.ucla.edu/>.
34. UCLA Depression Grand Challenge | Resilience Peer Network (RPN): Innovation to deliver needed care. <https://grandchallenges.ucla.edu/happenings/2016/01/18/resilience-peer-network/>.
35. UCLA Depression Grand Challenge. https://depression.semel.ucla.edu/studies_landing.

36. Rosenberg, B. M., Kodish, T., Cohen, Z. D., Gong-Guy, E. & Craske, M. G. A Novel Peer-to-Peer Coaching Program to Support Digital Mental Health: Design and Implementation. *JMIR Ment Health* **9**, e32430 (2022).
37. DiMatteo, M. R., Lepper, H. S. & Croghan, T. W. Depression Is a Risk Factor for Noncompliance With Medical Treatment: Meta-analysis of the Effects of Anxiety and Depression on Patient Adherence. *Archives of Internal Medicine* **160**, 2101–2107 (2000).
38. Egilsson, E., Bjarnason, R. & Njardvik, U. Usage and Weekly Attrition in a Smartphone-Based Health Behavior Intervention for Adolescents: Pilot Randomized Controlled Trial. *JMIR Form Res* **5**, e21432 (2021).
39. Wainer, H., Dorans, N. J., Flaugher, R., Green, B. F. & Mislevy, R. J. *Computerized Adaptive Testing: A Primer*. (Routledge, 2000).
40. Hastie, T., Mazumder, R., Lee, J. D. & Zadeh, R. Matrix Completion and Low-Rank SVD via Fast Alternating Least Squares. *Journal of Machine Learning Research* **16**, 3367–3402 (2015).
41. Hoffman, G. E. & Schadt, E. E. variancePartition: interpreting drivers of variation in complex gene expression studies. *BMC Bioinformatics* **17**, (2016).
42. Bates, D., Mächler, M., Bolker, B. & Walker, S. Fitting Linear Mixed-Effects Models Using lme4. *Journal of Statistical Software* **67**, (2015).
43. Zou, H. & Hastie, T. Regularization and Variable Selection via the Elastic Net. *Journal of the Royal Statistical Society. Series B (Statistical Methodology)* **67**, 301–320 (2005).
44. stats-package: The R Stats Package. <https://rdr.io/r/stats/stats-package.html>.

45. Benjamini, Y. & Hochberg, Y. Controlling the False Discovery Rate: A Practical and Powerful Approach to Multiple Testing. *Journal of the Royal Statistical Society. Series B (Methodological)* **57**, 289–300 (1995).
46. Borger, J. N., Huber, R. & Ghosh, A. Capturing sleep–wake cycles by using day-to-day smartphone touchscreen interactions. *npj Digit. Med.* **2**, 1–8 (2019).

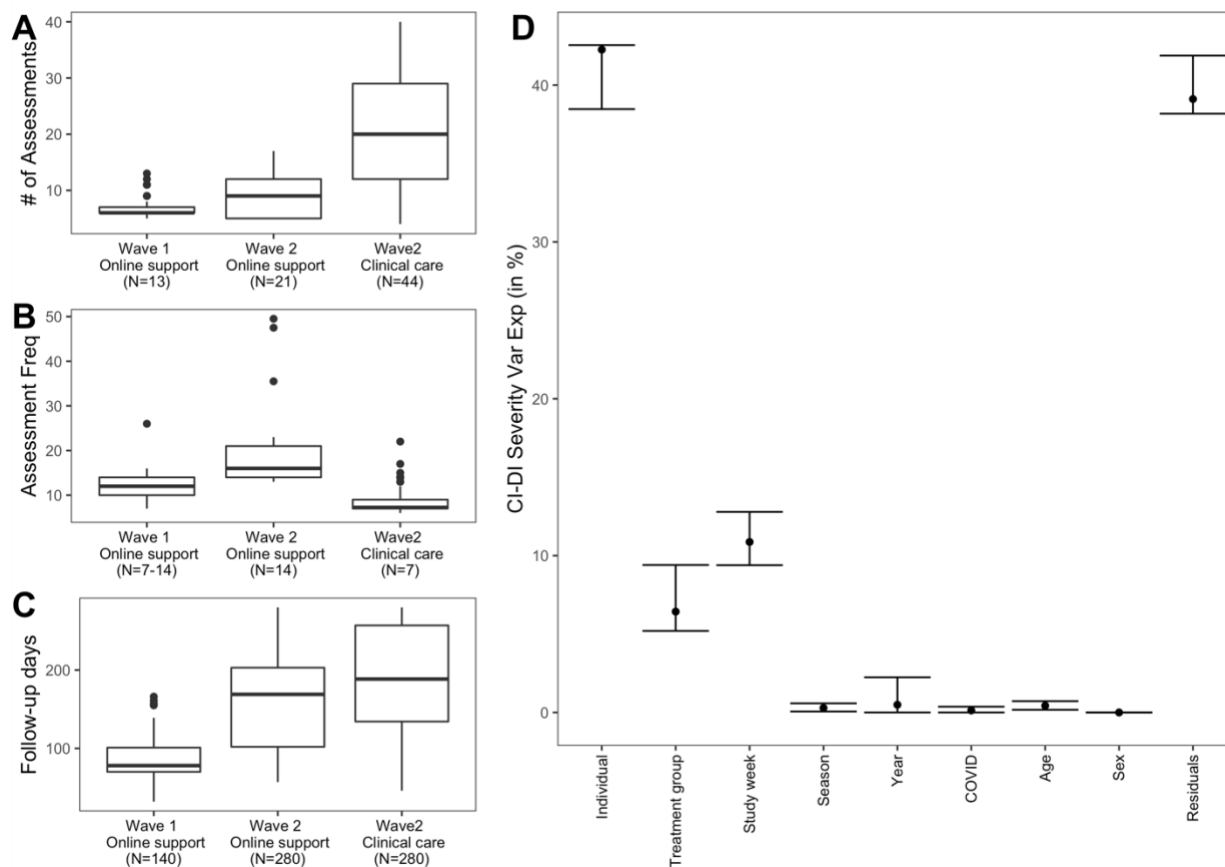


Figure 1: Overview of CAT-DI assessment frequency and source of variation in CAT-DI. (A-C) Boxplot of the observed number of CAT-DI assessments (B), follow-up time in days (C), and median number of days between assessments (D) for each wave and treatment group. The numbers in the parentheses indicate the expected values according to study design (Sup Figure 2). (D) Proportion of CAT-DI severity variance explained (VE) by inter-individual differences and other study parameters with 95% confidence intervals. The proportion of variance attributable to each source was computed using a linear mixed model with the individual id, treatment group, season, year, and sex modeled as random variables and all other variables modeled as fixed (see Online Methods).

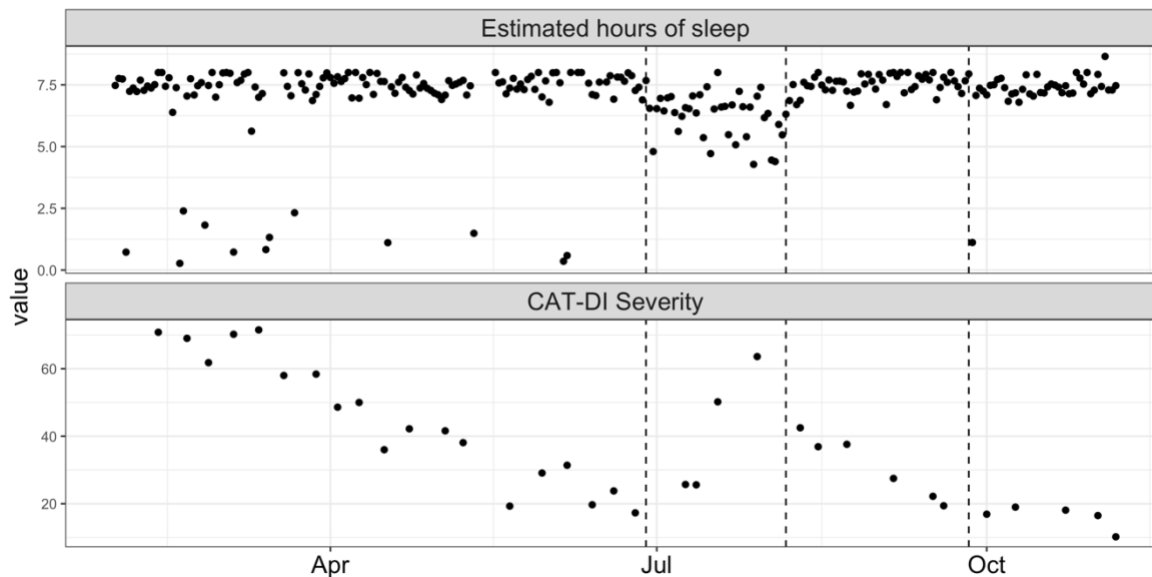


Figure 2: Example of identifying window of potential sleep disruption using sensor data related to phone usage and screen on/off status. The top panel shows estimated hours of sleep for an individual during the study while the bottom panel shows the depression severity scores during the same period. The dotted lines indicate the dates at which a change point is estimated to have occurred in the estimated hours of sleep as estimated using a change point model framework for sequential change detection (Online Methods).

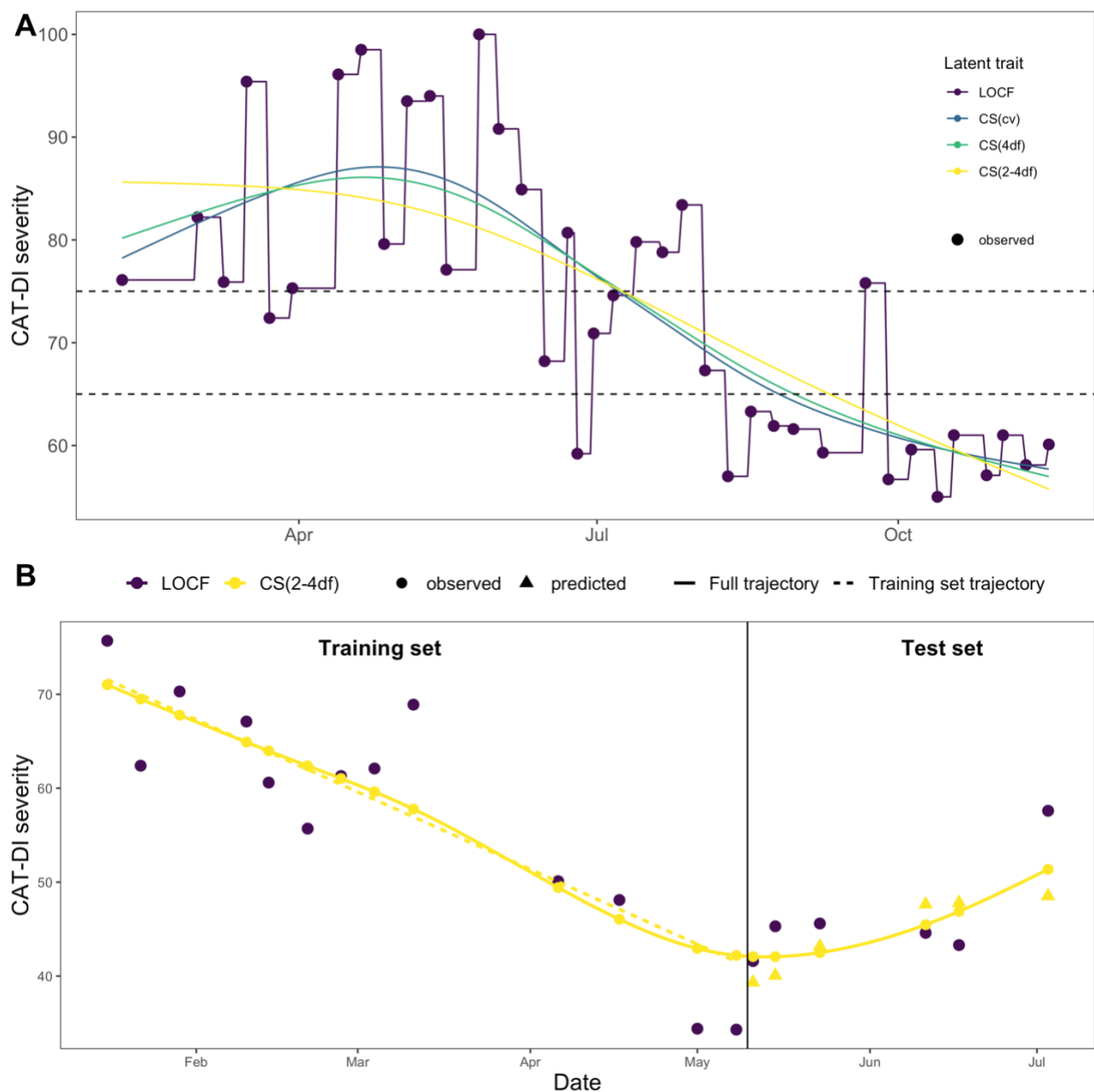


Figure 3: Interpolation of depression severity scores and latent trait inference. (A) Illustration of different interpolation methods considered for imputing the depression severity scores and inferring the latent depression traits. The dashed horizontal lines indicate the depression severity score thresholds for the mild and severe depression severity categories. (B) Illustration of the prediction method. We first infer the latent trait on the full CAT-DI trajectory of an individual (continuous yellow line). We then split the trajectory into a training set (days 1 until t) and a test set (days $t+1$ until T), infer the latent trait on the training set (dashed yellow line), and predict the trajectory in the test set (yellow triangles). Finally, we compute prediction accuracy metrics by comparing the observed (yellow circles) and predicted (yellow triangles) depression scores in the test set. The vertical line indicates the first date of the test set trajectory, i.e., the last 30% of the trajectory. LOCF: last observation carried forward. CS(x df): cubic spline with x degrees of freedom. CS(cv): best-fitting cubic spline according to leave-one-out cross-validation.

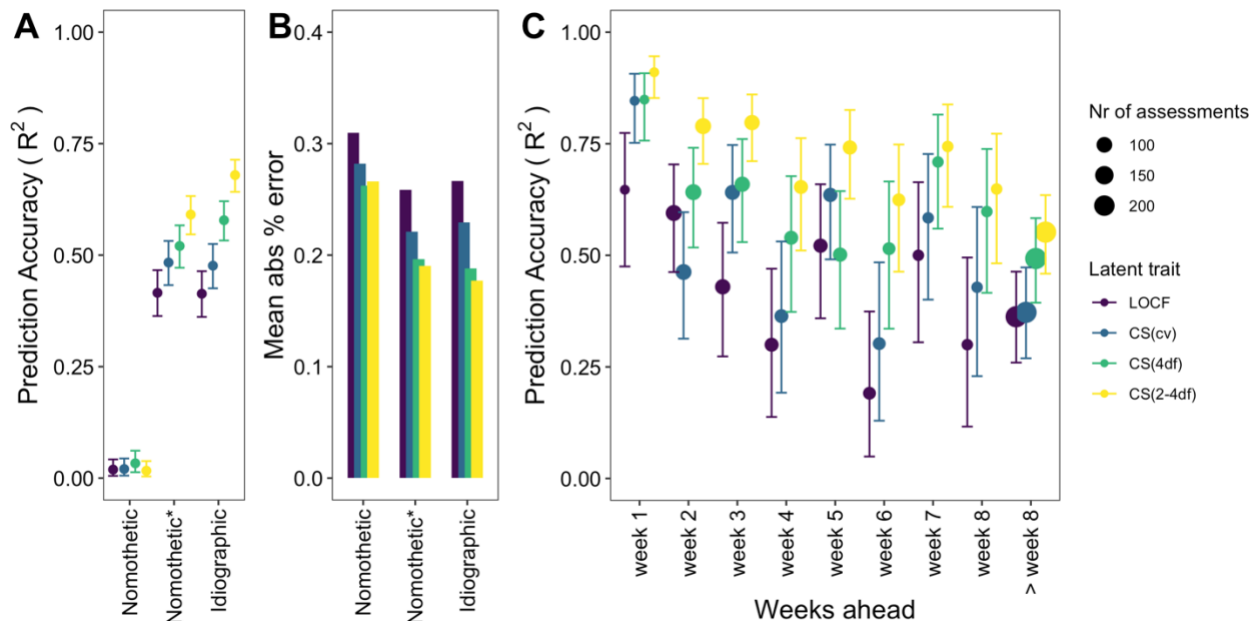


Figure 4: Idiographic models achieve higher group level prediction accuracy than nomothetic models. (A-B) CAT-DI prediction accuracy in the test set as measured by R^2 (A) and mean absolute percent error (B) across all individuals from the idiographic and two nomothetic models for different latent depression traits. (C) Prediction accuracy versus the number of weeks ahead we are predicting from the last observation in the training set. Each dot indicates the prediction accuracy and bars indicate 95% confidence intervals. The color indicates the different interpolation methods considered for imputing CAT-DI scores. The size of the dots indicates the number of CAT-DI measurements we predict each week. The dotted line indicates 80% prediction accuracy. MAE: mean absolute error. LOCF: last observation carried forward. CS(xdf): cubic spline with x degrees of freedom. CS(cv): best-fitting cubic spline according to leave-one-out cross-validation.

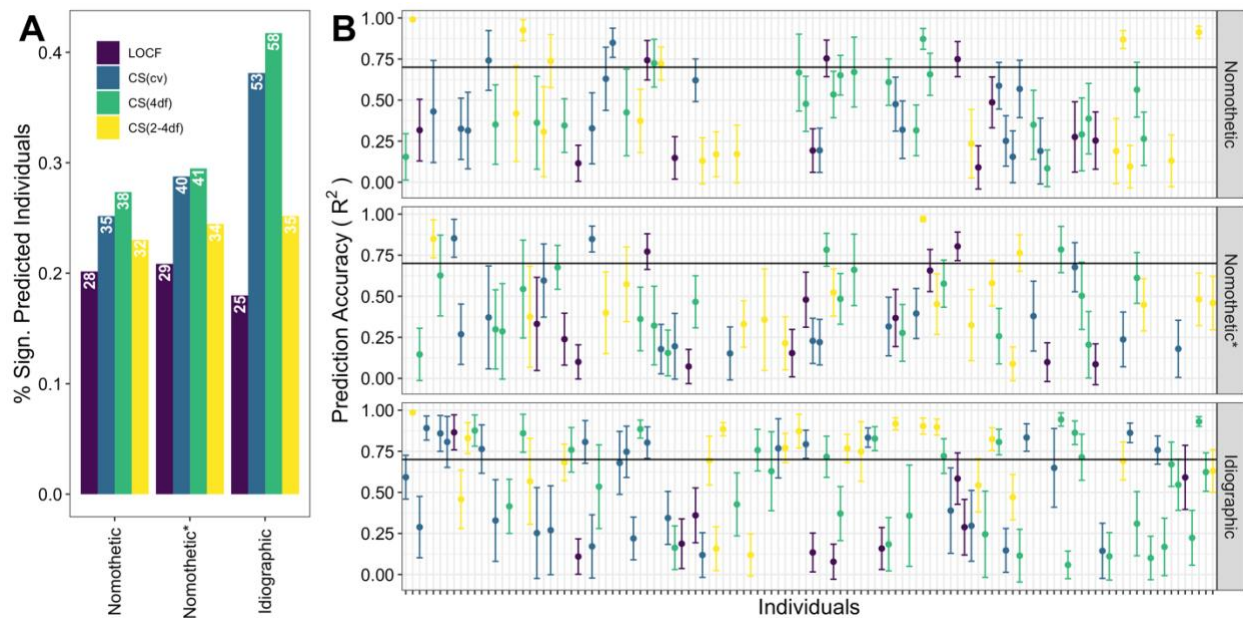


Figure 5: Idiographic models achieve higher individual level prediction accuracy than nomothetic models. (A) Bar plots of the proportion of individuals with significantly predicted mood ($FDR < 5\%$ and $R > 0$) for each latent trait and prediction model. Computed across individuals with at least five assessments in the test set ($N = 139$). Sup Figure 9 shows the overlap of significantly predicted individuals across different latent traits and prediction models. (B) Prediction accuracy (R^2) with 95% CI for best predicted latent trait across all significantly predicted individuals ($N = 118$, $FDR < 5\%$ and $R > 0$). Sup Figure 10 contains results for each latent trait. LOCF: last observation carried forward. CS(xdf): cubic spline with x degrees of freedom. CS(cv): best-fitting cubic spline according to leave-one-out cross-validation.

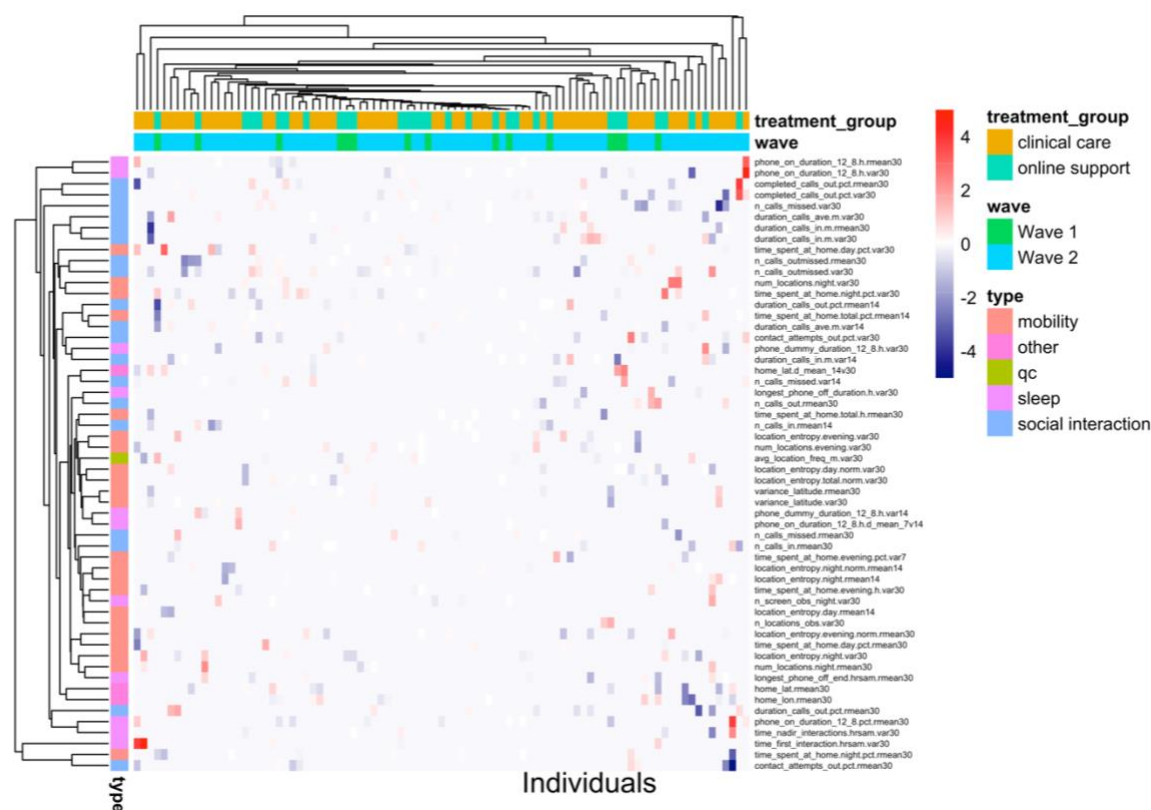


Figure 6: *Most predictive behaviors for CS(4df) latent trait according to idiographic models. Heatmap of idiographic elastic net regression coefficients for significantly predicted individuals ($N=91$ with $FDR<5\%$ and $R>0$). Columns indicate different individuals and rows indicate different features. To aid interpretation, we limit plot to features that are significant for at least two individuals and have an absolute coefficient value above one in at least one participant. The heatmap color indicates the elastic net coefficient for each feature and individual.*

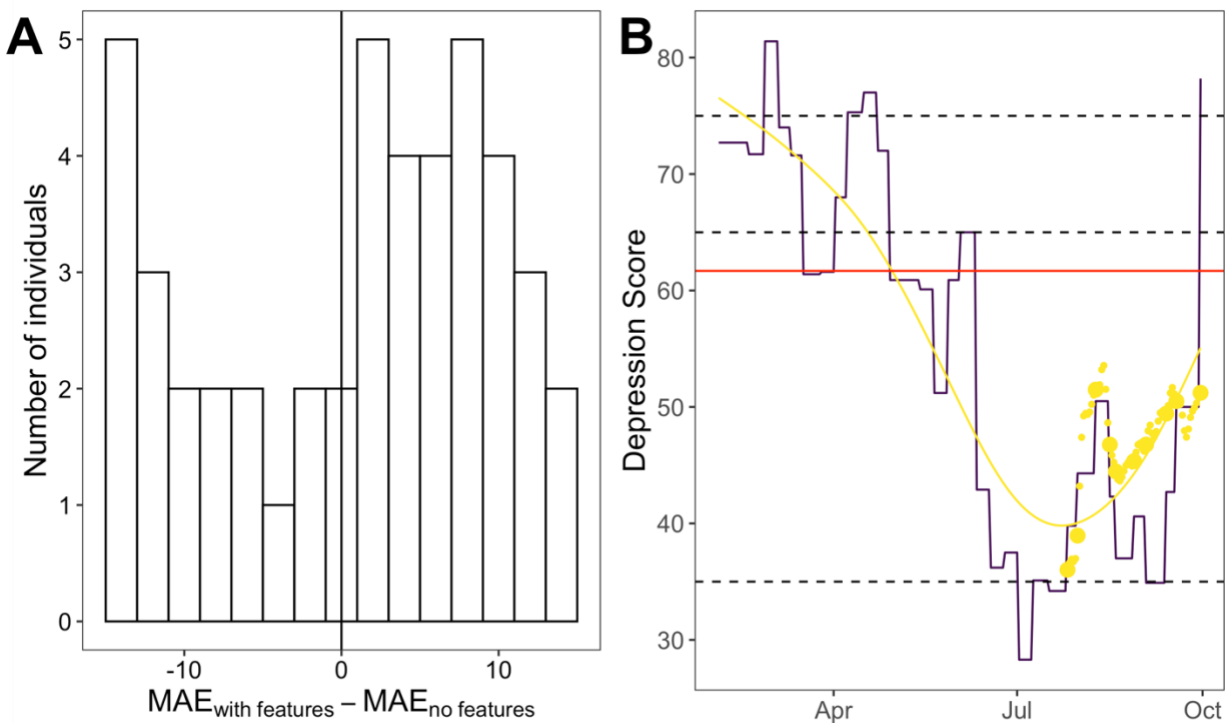


Figure 7: Comparison of the feature-based prediction model to a baseline prediction model. (A) Histogram of difference for each individual in mean absolute prediction error (MAE) between a baseline model that predicts based on past depression severity alone and a feature-based model which predicts based on past severity and past feature values. Negative values correspond to a decrease in prediction error when a prediction model with features is used, compared to the baseline model. **(B)** Prediction performance for an individual in our study for which features reduce the mean absolute prediction error of a baseline model by more than 10%. The lines indicate the observed LOCF (dark blue line) and cubic-spline interpolated (yellow line) CAT-DI scores for an individual in our study. The yellow dots are the predictions in the test set (30% of the time series; last six depression scores, two months ahead). The red line is the prediction of the baseline model which corresponds to the mean depression in the training set.

treatment group	0	-0.18	0.02
wave	0.1	-0.01	0.15
sex	-0.03	0.05	-0.06
age	0.14	-0.13	-0.11
# unique CAT-DI categories in test set	-0.17	0.26	0.17
# unique CAT-DI categories in training set	0.28	0.46	-0.05
# unique CAT-DI categories total	0.11	0.55	-0.11
difference in CAT-DI severity b/w training and test set	0.01	0.65	-0.54
# CAT-DI assessment in test set	-0.18	0.13	-0.04
# CAT-DI assessment in train set	-0.17	0.11	-0.01
	R^2	MAE	MAE_{diff}

Figure 8: Factors associated with prediction performance of CAT-DI severity scores. Correlation between prediction accuracy of an individual (metrics on the y-axis) and the number of CAT-DI assessment available in the training and test set, the difference in median CAT-DI severity between the training and test set, the number of the unique CAT-DI categories (normal to severe) observed (total and in training and test sets), age, sex, wave, and treatment group (a proxy for depression severity). MAE: mean absolute error of the feature-based model. MAE_{diff} : mean absolute error difference between the feature-based and baseline models of each individual, i.e., $MAE_{features} - MAE_{no\ features}$.

Supplementary information

Feature extraction from smartphone sensors

Preprocessing features

Each sensor collected through the AWARE framework is stored separately with a common set of data items (device identifier, timestamp, etc.) as well as a set of items unique to each sensor (sensor-specific items such as GPS coordinates, screen state, etc.). Data from each sensor was preprocessed to convert Unix UTC timestamps into local time, remove duplicate logging entries, and remove entries with missing sensor data. Additionally, some data labels that are numerically coded during data collection (e.g., screen state) were converted to human-readable labels for ease of interpretation.

Mobility features

Location data was divided into 24-hour windows starting and ending at midnight each day. To identify locations where participants spent time, GPS data were filtered to identify observations where the participants were stationary since the previous observation. Stationary observations were those defined as having an average speed of <0.7 meters per second (approximately half the average walking speed of the average adult). These stationary observations were then clustered using hierarchical clustering to identify unique locations in which participants spent time during each day. Hierarchical clustering was chosen over k-means

and density-based approaches such as DBSCAN due to its ability to deterministically assign clusters to locations with a precisely defined and consistent radius, independent of occasional data missingness.

Locations were defined to have a maximum radius of 400 m, a sufficient radius to account for noise in GPS observations. Clusters were then filtered to exclude any location in which the participant spent less than 15 minutes over the day to exclude location artifacts, e.g., a participant being stuck in traffic during daily commute, or passing through the same area of campus multiple times in a day. To address data missingness in situations where GPS observations were not received at regular intervals, locations were linearly interpolated to provide an estimated location every 3 minutes.

For each day, a home location was assigned based on the location each participant spent the most time in between the hours of midnight to eight am. This approach allowed for better interpretation of behavior for participants who split time between multiple living situations, for example, students who return home for the weekend or a vacation. Next, multiple features were extracted from this location data, including total time spent at home each day, total number of locations visited, overall location entropy, and normalized location entropy. Each of these features was additionally computed over three daily non-overlapping time windows of equal duration (night 00:00-08:00, day 08:00-16:00, evening 16:00-00:00), under the hypothesis that participant behavior may be more or less variable based on external constraints such as a regular class schedule during daytime hours. In total, 28 mobility features were extracted.

Sleep and circadian rhythm features

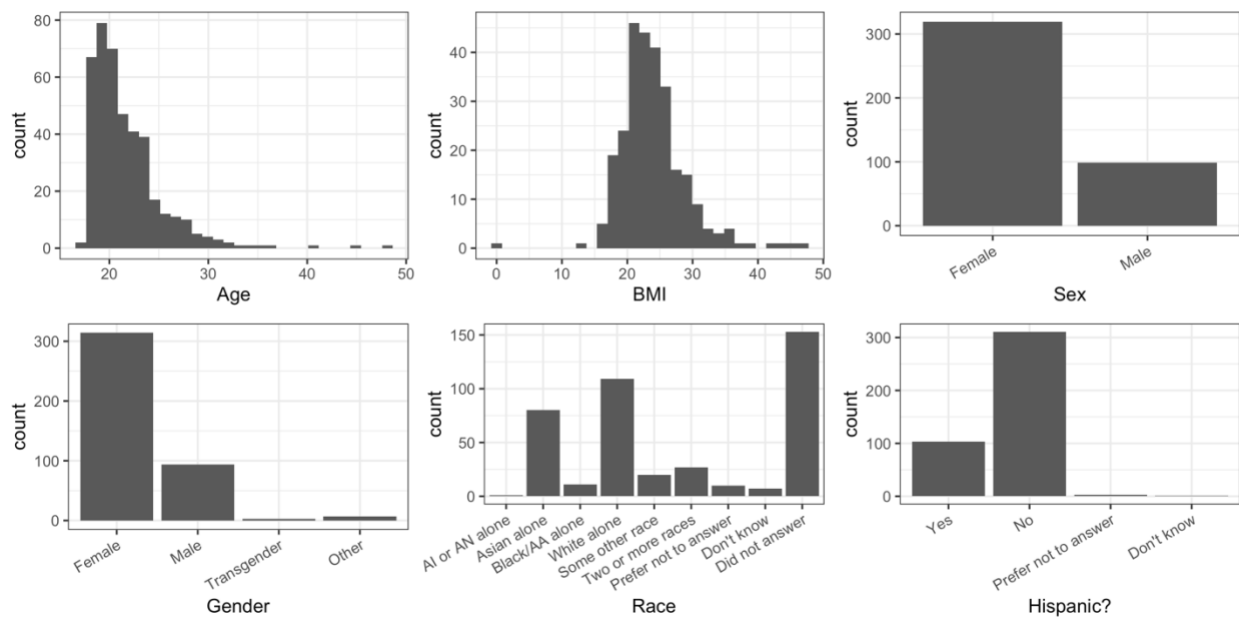
Sleep and circadian rhythm features were extracted from logs of participant interactions with their phone, following prior work showing that last interaction with the phone at night can serve as a reasonable proxy for bedtime, and first interaction in the morning for waketime⁴⁶. The longest phone-off period (or assumed uninterrupted sleep duration) was tracked each night, as well as the beginning and end time of that window as estimates of bedtime and waketime. To account for participants who may have interrupted sleep, the time spent using the phone between the hours of midnight and 8 am was also tracked to account for participants who may use their phone briefly in the middle of the night but are otherwise asleep for the majority of that window. Finally, time-varying kernel density estimates were derived using the total set of phone interactions, to estimate the daily time nadir of interactions, as an additional proxy for the time of overall circadian digital activity nadir. In total, 12 sleep and circadian rhythm features were extracted.

Social interaction and other device usage features

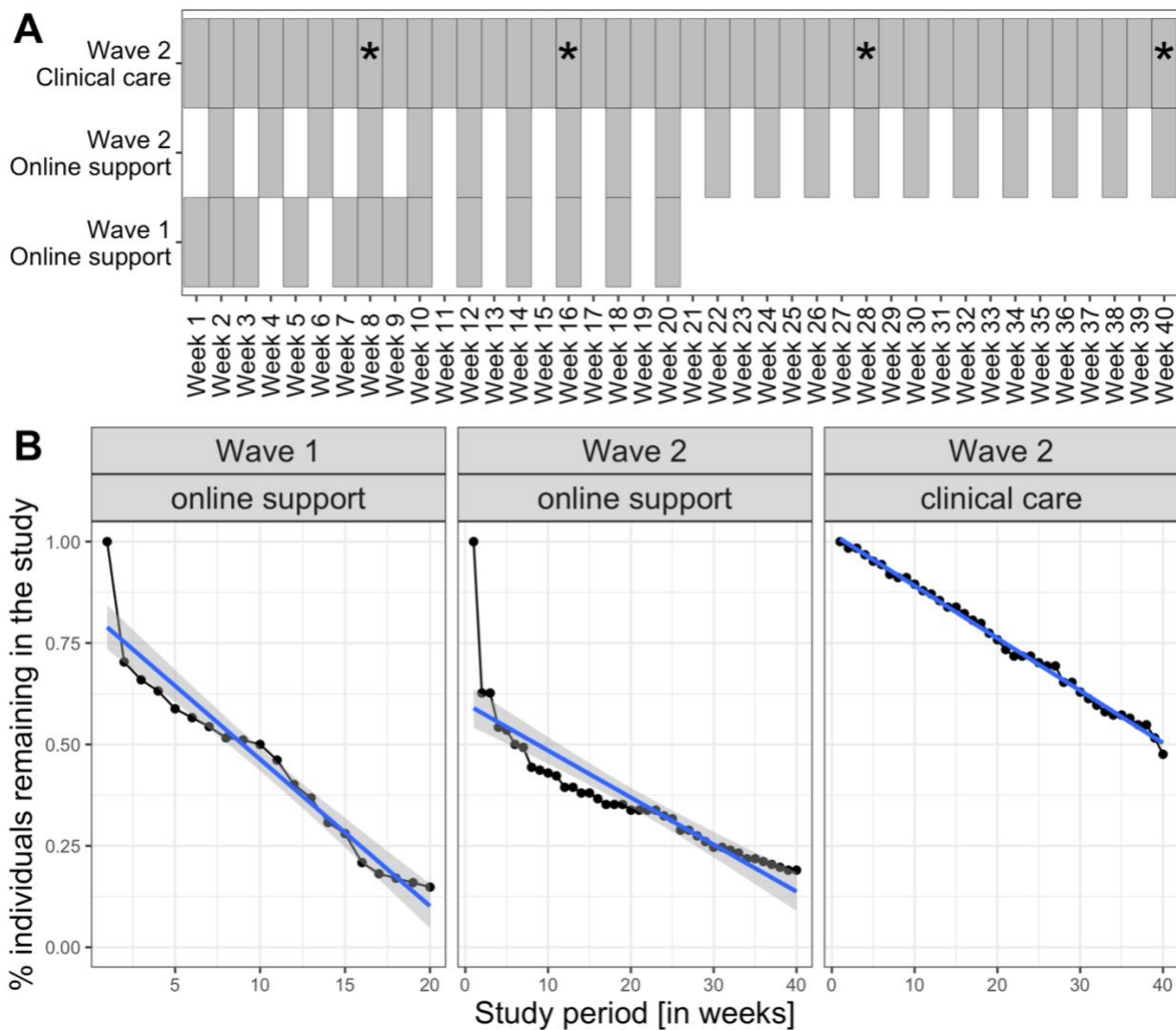
Additional social interaction features were extracted from anonymized logs of participant calls and text messages sent and received from their smartphone device. Features extracted from this data include, for example, the total number of phone calls made, total time spent on the phone, and percentage of calls connected that were outgoing (i.e., dialed by the participant) versus incoming. In total, 18 social interaction and device usage features were extracted. Due to OS restrictions, sensors needed to extract text message features are not available on iOS devices and were only computed for the 15 participants with Android devices.

Mapping of behavioral features to DSM-5 Major Depressive Disorder criteria

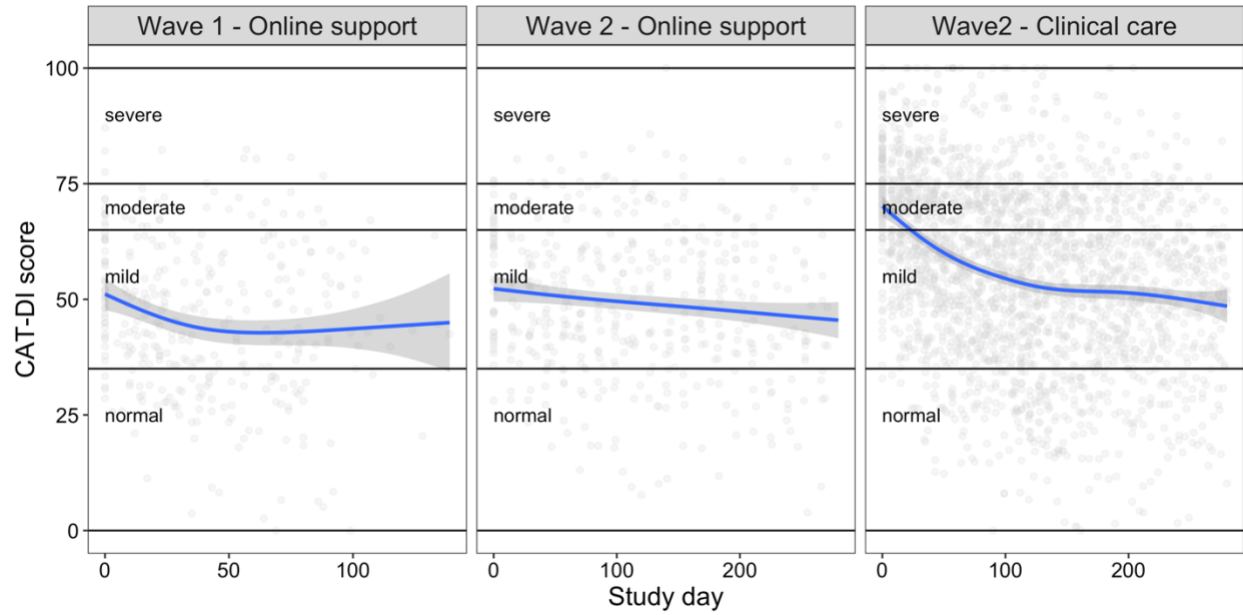
The set of features described above map onto only a subset of DSM criteria that are closely associated with externally observable behaviors (Sup Figure 5) - sleep, loss of energy, and anhedonia (to the extent it is severe enough to globally reduce self-initiated activity). Other DSM criteria such as weight change, appetite disturbance, and psychomotor agitation/retardation are in theory also directly observable, but less so with the set of sensors available on a standard smartphone. For these criteria, other device sensors - for instance, smartwatch sensors - may be more applicable in the detection of e.g., fidgeting associated with psychomotor agitation. A final set of DSM criteria include those primarily subjective findings - depressed mood, feelings of worthlessness, suicidal ideation - which inherently require self-report to directly assess. Given that only 5 of 9 criteria are required for the diagnosis of MDD, an individual patient's set of symptoms may overlap minimally with those symptoms we expect to measure with the features described above. However, for others, the above features may cover a more significant portion of their symptom presentation and do a better job directly quantifying fluctuations in DSM-5 criteria for that individual.



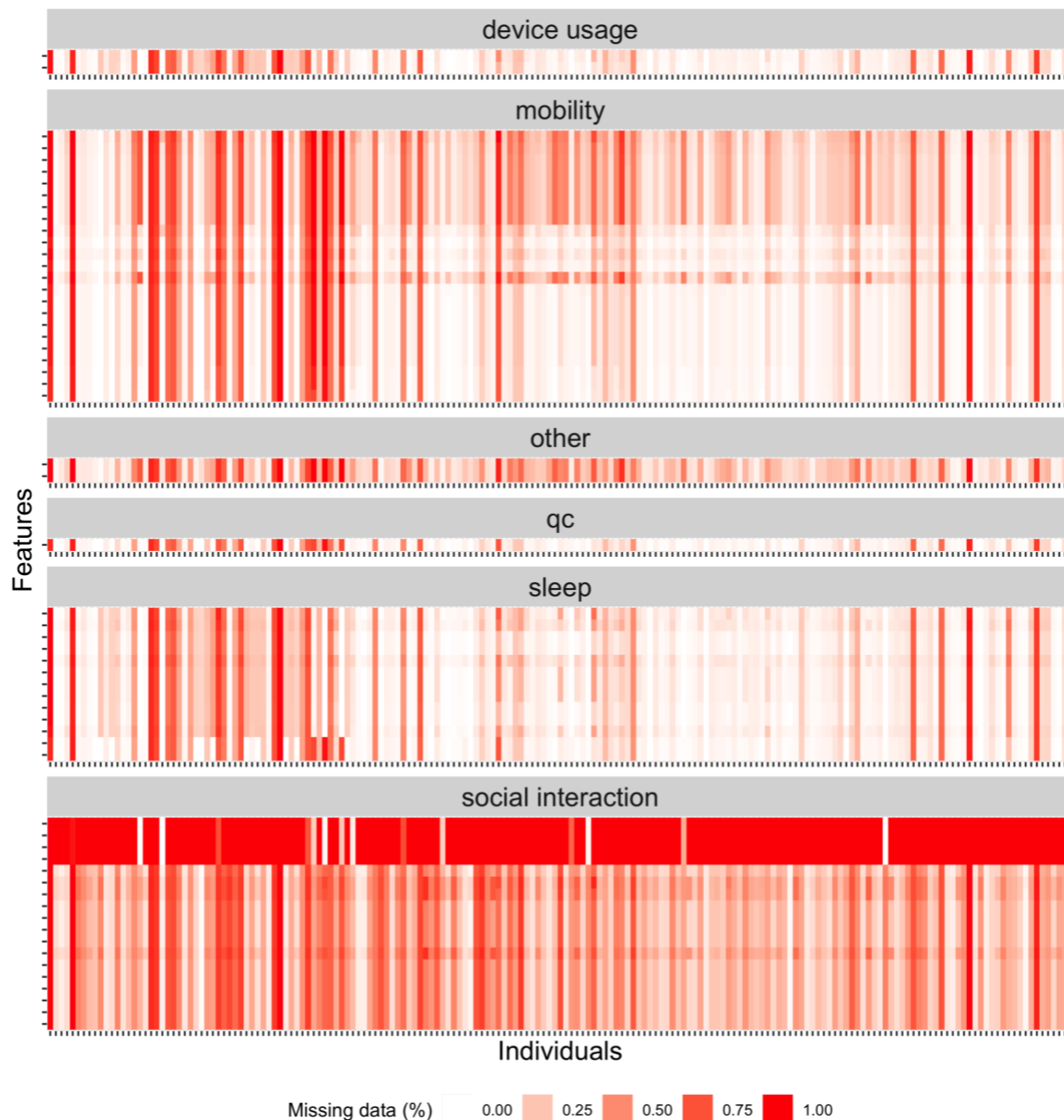
Sup Figure 1: **Demographic information for participants in each wave.** First row: histogram of age and BMI and bar plot of sex. Second row: bar plot of gender, race, and ethnicity. AI or AN: American Indian or Alaska Native. AA: African American.



Sup Figure 2: CAT-DI administration protocol and compliance with CAT-DI assessment protocol for each wave and treatment group. (A) CAT-DI administration schedule. Each box indicates a week during which participants in each group were expected to complete the CAT-DI. Asterisks indicate weeks with additional in-person administrations of CAT-DI for Wave 2 participants which received clinical care. (B) Participant CAT-DI retention rate for each enrollment wave and treatment group. The x-axis shows weeks from the beginning of the study for each participant while the y axis shows the proportion of individuals that were still completing the CAT-DI at that week. The continuous lines show the linear regression fit with 95% confidence intervals (gray shading).



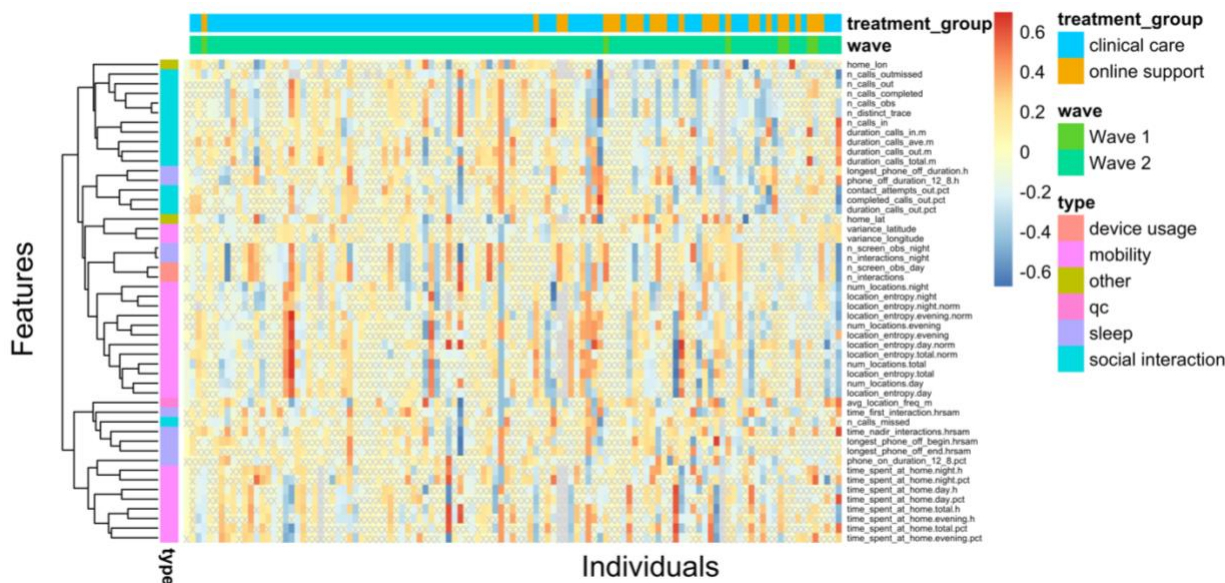
Sup Figure 3: **Effect of therapy per wave and treatment group.** The x-axis shows the study day with zero indicating the first day of CAT-DI assessment for each individual. The y-axis indicates the CAT-DI severity score for each individual / day in the study. The blue line indicates the fit of a generalized additive model with $y \sim s(\text{day} + \text{wave: treatment group}, \text{bs} = "cs")$ and gaussian family.



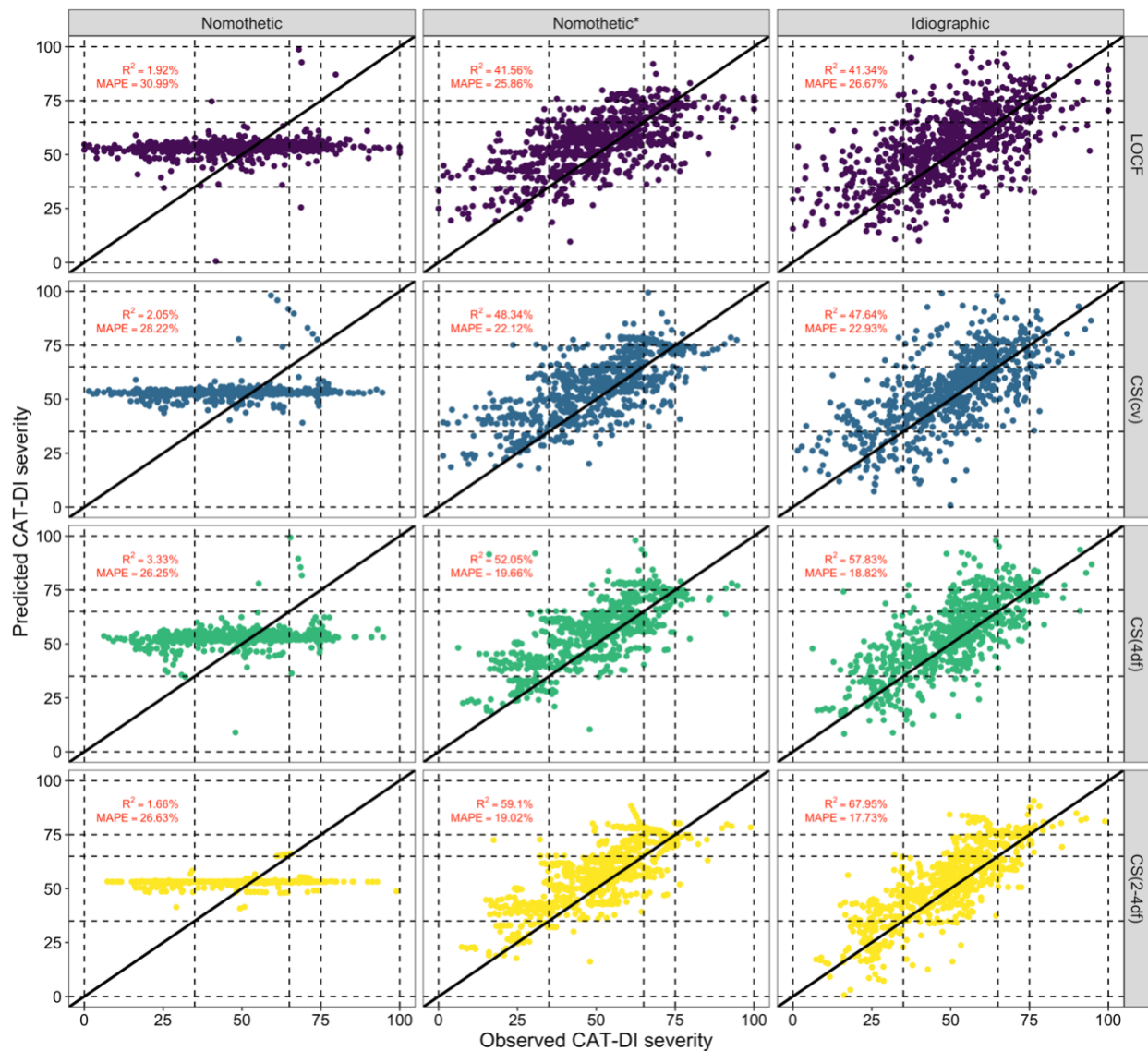
Sup Figure 4: Missing feature data summary. Heat map showing missing data percentage in each of the four types of features extracted from smartphone data for all individuals. Each tick on the x-axis (y-axis) represents an individual (feature). For ease of plotting, we have excluded transformation-based features. For participants with iOS devices (majority of individuals), we did not have any information on social interaction features related to text message information due to permission. These features are excluded from analyses when considering individuals with iOS devices.

		Depressed mood	Diminished interest or loss of pleasure activities (anhedonia)	Weight change or appetite disturbance	Sleep disturbance	Psycho motor agitation or retardation	Fatigue or loss of energy	Feelings of worthlessness	Diminished concentration; indecisiveness	Suicidal ideation/intent
Mobility features	Variance in latitude		•							
	Variance in longitude		•							
	Number of locations visited in total		•							
	Number of locations visited at night		•							
	Number of locations visited during the day		•							
	Number of locations visited in the evening		•							
	Location entropy over full day		•							
	Location entropy over full day (normalized)		•							
	Location entropy at night		•							
	Location entropy at night (normalized)		•							
	Location entropy during the day		•							
	Location entropy during the day (normalized)		•							
	Location entropy in the evening		•							
	Location entropy in the evening (normalized)		•							
	Time spent at home total (hours)		•				•			
	Time spent at home at night (hours)		•				•			
	Time spent at home during the day (hours)		•				•			
	Time spent at home in the evening (hours)		•				•			
	Percentage of time spent at home in total (%)		•				•			
	Percentage of time spent at home at night (%)		•				•			
Percentage of time spent at home during the day (%)		•				•				
Percentage of time spent at home in the evening (%)		•				•				
Phone interactions	Number of phone interactions during day							•		
	Number of phone interactions at night				•					
Sleep	Duration of longest phone off period (hours)				•					
	Beginning of longest phone off period				•					
	End of longest phone off period				•					
	Phone on duration midnight to 8am (hours)				•					
	Phone off duration midnight to 8am (hours)				•					
	Percentage of time phone on midnight to 8am (%)				•					
	Time of nadir of phone interactions				•					
Social interaction	Total number of calls		•							
	Number of incoming calls attempted		•							
	Number of outgoing calls attempted		•							
	Number of completed calls		•							
	Number of missed calls		•							
	Number of unanswered outgoing calls		•							
	Percentage of completed outgoing calls (%)		•							
	Percentage of unanswered outgoing calls (%)		•							
	Duration of incoming calls (minutes)		•							
	Duration of outgoing calls (minutes)		•							
	Total time spent on phone (minutes)		•							
	Average duration per call (minutes)		•							
	Duration of outgoing calls (%)		•							
	Number of distinct message contacts		•							
	Total number of messages		•							
	Number of incoming messages		•							
	Number of outgoing messages		•							
Percent of messages outgoing		•								

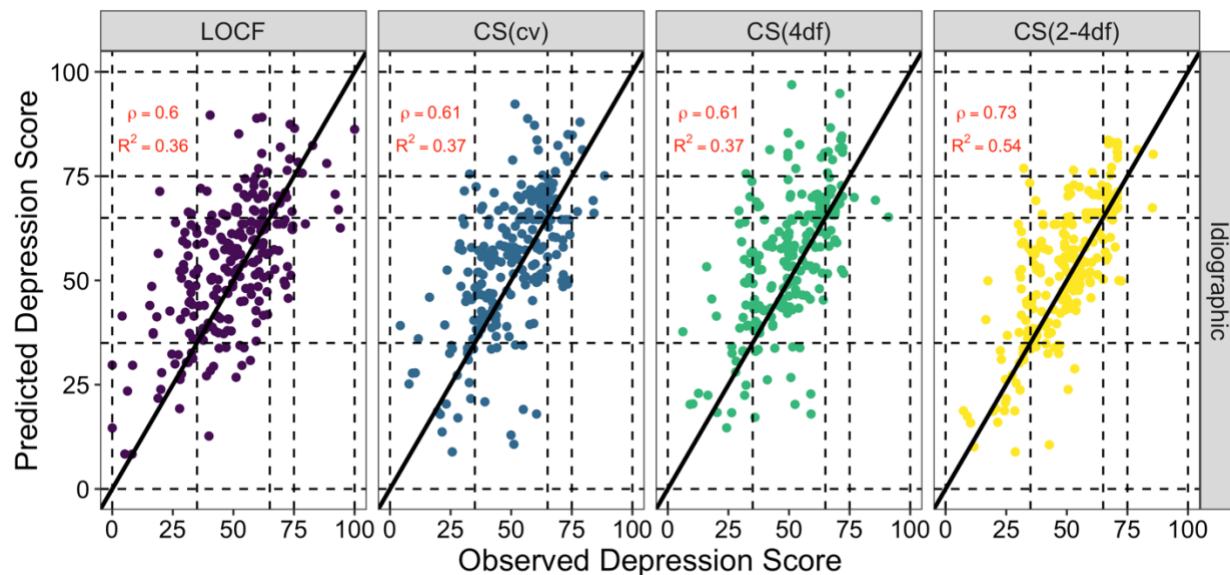
Sup Figure 5: **Mapping of sensor-derived behavioral features to DSM5 Major Depressive Disorder criteria.** The individual behavioral features derived from phone sensors map primarily to the DSM criteria of disrupted sleep, loss of energy, and anhedonia. Each of these base features is further transformed to look for deviations from individual baseline over varying time scales (e.g., last day's deviation from the weekly average) to arrive at the final set of behavioral features.



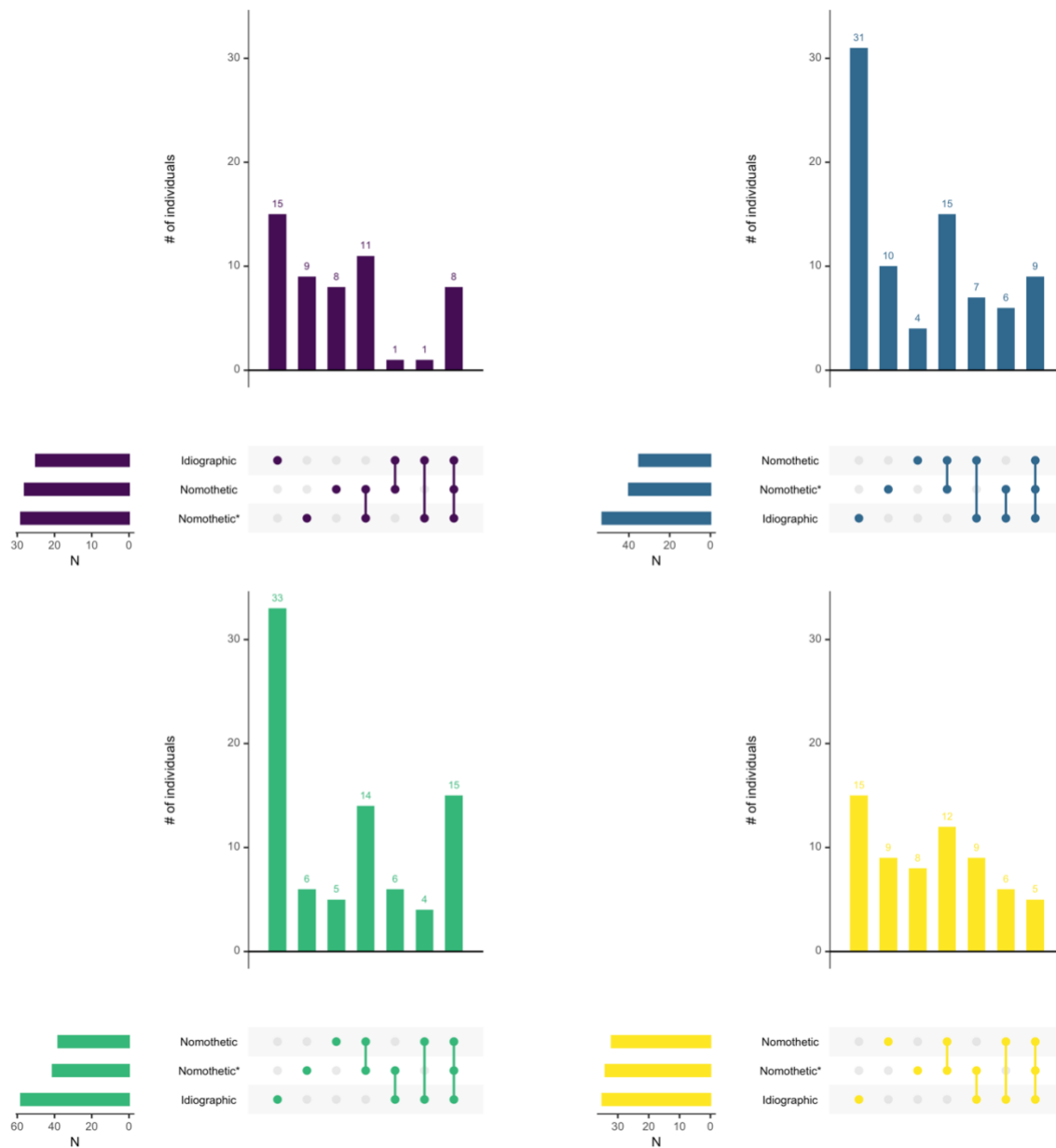
Sup Figure 6: **Correlation between depression severity scores and features within each individual and across individuals.** Heatmap for Pearson's correlation coefficient (color of cell) between CAT-DI scores and behavioral features (y-axis) across individuals (first column) and within each individual (x-axis). Correlation coefficients with nominal p-values > 0.05 are indicated by x. For plotting ease, we limit to untransformed features (N=50, see Online Methods). Rows and columns are annotated by feature type and by each individual's wave and treatment group.



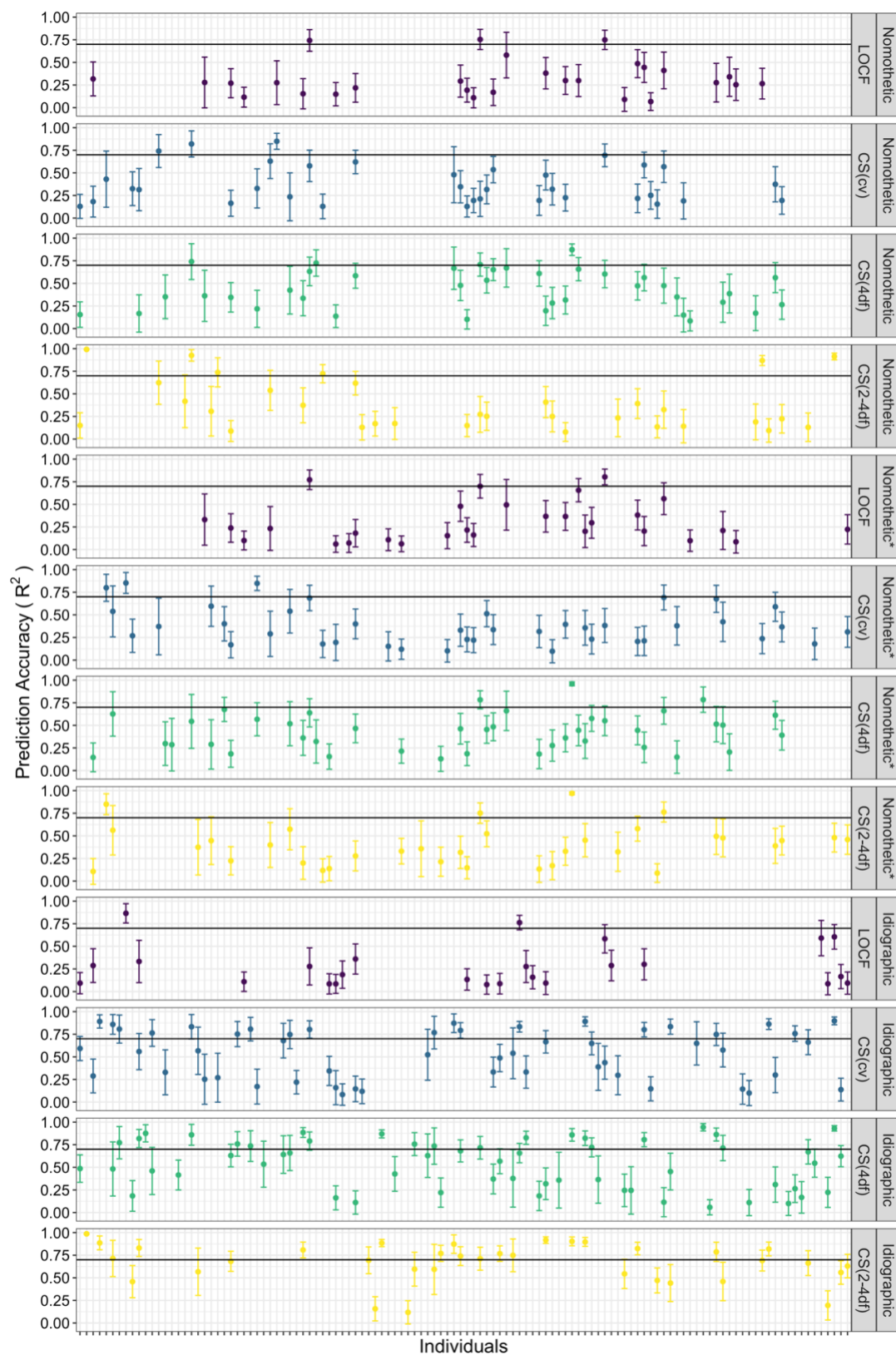
Sup Figure 7: **Idiographic models achieve higher prediction accuracy than nomothetic models across individuals.** Observed versus predicted CAT-DI scores in the test set from the idiographic and two nomothetic models for different latent depression traits. MAPE: mean absolute percent error. LOCF: last observation carried forward. CS(cv): best-fitting cubic spline according to leave-one-out cross-validation. CS(xdf): cubic spline with x degrees of freedom.



Sup Figure 8: **Prediction performance when features are imputed using matrix completion (softImpute).** Observed versus predicted CAT-DI scores in the test set from the idiographic model for different latent depression traits. MAPE: mean absolute percent error. LOCF: last observation carried forward. CS(cv): best-fitting cubic spline according to leave-one-out cross-validation. CS(xdf): cubic spline with x degrees of freedom.



Sup Figure 9: **Idiographic models achieve higher prediction accuracy than nomothetic models within individuals.** Upset plots of the number of individuals significantly predicted ($FDR \leq .05$ and $R > 0$) using the idiographic and two nomothetic models for different latent depression traits.



Sup Figure 10: **Idiographic models achieve higher prediction accuracy than nomothetic models within individuals.** Prediction accuracy (R^2) for all significantly predicted individuals ($FDR \leq .05$ and $R > 0$) using the idiographic and two nomothetic models for different latent depression traits.